Title

Forcing the issue: testing gecko-inspired adhesives

Journal

Journal of The Royal Society Interface, 18(174)

ISSN

1742-5689

Authors

Suresh, Srinivasan A
Hajj-Ahmad, Amar
Hawkes, Elliot W
et al.

Publication Date

2021

DOI

10.1098/rsif.2020.0730

Peer reviewed

Forcing the issue: testing gecko-inspired adhesives

Srinivasan A. Suresh[a,1], Amar Hajj-Ahmad[a], Elliot W. Hawkes[b], Mark R. Cutkosky[a]
[1]To whom correspondence should be addressed: sasuresh@alumni.stanford.edu
[a]Department of Mechanical Engineering, Stanford University, Stanford, CA 94305, USA
[b]Department of Mechanical Engineering, University of California, Santa Barbara, CA, 93106, USA

***Abstract*—Materials are traditionally tested either by imposing controlled displacements and measuring the corresponding forces, or by imposing controlled forces. The first of these approaches is more common because it is straightforward to control the displacements of a stiff apparatus and, if the material suddenly fails, little energy is released. However, when testing gecko-inspired adhesives, an applied force paradigm is closer to how the adhesives are loaded in practice. Moreover, we demonstrate that the controlled displacement paradigm can lead to artifacts in the assumed behavior unless the imposed loading trajectory precisely matches the deflections that would occur in applications. We present the design of a controlled-force system and protocol for testing directional gecko-inspired adhesives and show that results obtained with it are in some cases substantially different from those with controlled-displacement testing. An advantage of the controlled-force testing approach is that it allows accurate generation of adhesive limit curves without prior knowledge of the expected behavior of the material or the loading details associated with practical applications.**

***Index Terms*—gecko-inspired adhesives, microstructures, materials, testing.**

I. Introduction

THE last 20 years have seen considerable interest in bioinspired dry adhesives, based on discoveries regarding the adhesive system of the gecko and some arthropods [1]–[4]. Desirable properties of such adhesives are that they leave no residue when detached, are reusable for many cycles, and can be controllable—not sticky in their default state but providing useful levels of adhesion or friction when loaded appropriately. Synthetic adhesives have been created with a range of properties. Some require a relatively high preload to make initial contact but then provide high levels of adhesion and friction. These adhesives also require substantial effort to detach or peel for removal [5]–[7]. Others require essentially no normal force to engage with a surface, but adhere and release in response to the magnitude of an applied shear force [8], [9]. Recent reviews include [10]–[17].

The variety of gecko-inspired adhesives has found a similar variety of applications, from robotic and human climbing [18]–[21], to grasping fragile objects [22], [23], to attaching sensors [24]. Each of these applications may impose different requirements but they all benefit from metrics and a testing protocol that reliably predicts performance under a range of conditions.

The predominant method of gathering the data used to evaluate adhesives and to design systems that exploit them is to contact the adhesive to a test surface, apply a displacement, and measure the resulting force. While this displacement-controlled method is common in materials testing (e.g. [25]), in the case of gecko-inspired adhesives it can lead to a mismatch between the testing methodology and the in-use loading state. As gecko-inspired adhesives depend on the geometry of the microstructure for their adhesive properties, the particular deformations of the structure as it is loaded can significantly affect adhesion. Performing testing in displacement-controlled conditions can impose geometric deformations that would not be seen in applications, resulting in a mismatch. While it is certainly possible for gecko-inspired adhesives to have force capabilities that depend on geometric deformations—indeed, the gecko itself requires shear motion to fully engage the adhesive [26]—it is important that the testing methodology does not introduce additional deformations that are due only to the testing method. In this paper, we show that for directional gecko-inspired adhesives, displacement-controlled testing introduces such effects, which can lead to incorrect predictions about adhesive behavior. While in some cases this mismatch between test and use can be unimportant, or masked by non-ideal loading of the adhesive, we show that for at least one case of a directional adhesive, the mismatch predicts a lack of adhesion for some conditions under which significant adhesion is available.

In the following sections we discuss the aspects of test methodology that affect the mapping between measured and real-world performance. We present a new test apparatus and testing protocol that improve on commonly used methods, and present data comparing measurements obtained by varying the test control variable and path.

We show that testing gecko-inspired adhesives under force-controlled rather than displacement-controlled conditions reduces added path dependence, tests the material under conditions relevant to practical applications, and yields data that can be used with confidence when designing systems which employ these adhesives under a variety of expected conditions.

II. Background

A variety of techniques have been used to characterize gecko-inspired adhesives, many of which are discussed in [17]. Tests can be performed on very small samples (e.g. a single setal stalk [27]) or on large samples that are built into a system (e.g. [7], [28]–[31]). Often, system tests are conducted on adhesives that have already been characterized at a small scale in bench-top tests. For all such tests, there are some basic

Manuscript compiled June 10, 2021.

distinctions that determine how directly the test conditions and data reflect loading in applications. These distinctions are summarized in Table I for several reported studies measuring adhesive strength. We discuss these in more detail below.

A. Force-Controlled vs Displacement-Controlled Testing

Adhesive characterization typically has the supported contact stress as the measure of interest, which in general has both normal and shear components.

Using a displacement-controlled testing method to determine the supported contact stress has several advantages. Since the system is stiff, measurements are highly repeatable, and the released energy at failure is well contained. This approach also offers precise control over strain rates, which is key for thoroughly characterizing the response of viscoelastic materials. Together, these make displacement-space testing an excellent option for developing small-scale theories of adhesion, where the two adherends are of simple, well understood geometry, such as for Hertzian contacts or simple film peeling.

However, when using gecko-inspired adhesives in applications—such as climbing robots or manipulation with adhesion—in nearly all cases the adhesive has forces applied to it, and not constrained displacements. Further, while many of the adhesives reported in the literature broadly correspond to well-understood geometries (e.g. flat punch or peeling models), they are loaded in more complex ways. Since gecko-inspired adhesives derive their properties directly from the microscopic surface features, and particularly from the behavior of these features (e.g. as they bend and flatten) when the adhesive is loaded, the deformation under load significantly affects the adhesion properties. This deformation is what gives the gecko its highly directional adhesion and is similarly responsible for the anisotropic behavior of many synthetic bioinspired adhesives. Even for adhesives not designed to be anisotropic, off-axis loading will cause deformation of the structure which may affect adhesion in ways that are hard to predict.

Despite these complexities of microscopic behavior, a common method of testing areas of gecko adhesive to predict performance in applications is use a stiff motion stage that applies controlled displacements to bring an adhesive into contact with a test surface and then pulls until adhesive failure is observed. While this has the benefit of being constrained and highly repeatable, it does not reflect real-world loading conditions, potentially leading to systematic errors when interpreting results. In particular, when using this testing method, the motion of the microscopic features is not governed by the geometry of the microstructure, but is imposed by the motion of the much stiffer motion stage. This leads to a significant effect of loading trajectory on the measured adhesion [52]. As a simple example, for the gecko, any trajectory that does not pull the setal stalks to align the spatular tips with a surface will record a low adhesion force [26].

In some cases, the displacement trajectory can be selected to approximate the unconstrained motion of the adhesive structure in a use case, but this may not be known in advance.

A second source of variation is force sensing. While many studies use a very stiff force sensor (e.g. [32], [33]), others use single or dual-axis cantilevers with comparatively low stiffness in comparison to a positioning stage [1], [27], [38], [41], [47], [48], [53]. While not all publications specify the cantilever stiffness, those that do often employ cantilevers that are stiffer than the adhesive itself, so that adhesive behavior remains dependent on the applied displacement trajectory. Where the force sensor is soft, one needs to consider the combined deflections of the adhesive and force sensor.

Displacement-controlled testing has a further disadvantage in the case of any microstructured adhesive that is loaded such that the macroscopic behavior arises from a sequence of deformation and engagement at the microscopic level. The most common case to date is that of adhesives designed to be highly anisotropic [54]. In cases of microstructures like this, approximating the unconstrained motion of the adhesive structure with an appropriate displacement trajectory becomes difficult without already having a high-fidelity model of the adhesive behavior. In particular, as seen in Section IV, for adhesives that can produce a substantial shear force when the normal force is essentially zero, a displacement-controlled trajectory has difficulty producing this condition.

Force-controlled testing avoids the foregoing difficulties by aligning test conditions to those typically encountered in use cases. This approach allows for repeatable, robust testing of adhesives without prior knowledge of the expected adhesive behavior. A common method is to employ a small patch of adhesive and use weights or a force scale to apply shear and/or normal loads [17]. Manual force application can also be extended to measuring full limit surfaces for an adhesive patch [55] as well as to measuring frictional forces by applying a weight to define a positive normal force [43], [54]. While manual loading avoids the issues of displacement-controlled testing, it is typically slow and the recorded data are limited to the forces associated with failure, making it difficult to estimate the work of adhesion or adhesive stiffness. Manual load application can also produce greater variation in the details of force direction and alignment, resulting in greater variability in recorded data.

Development of an automated force-controlled test apparatus can retain the benefits of force testing while improving data quality and ease of adhesive characterization. Ruffatto *et al.* have developed force-controlled test fixtures using pneumatics to apply controlled forces, including an apparatus to perform tests at specific angles on adhesives [36], and a uniaxial test apparatus to test adhesives in shear [46]. Although these investigations employ testing with applied forces, they do not present a generic force-controlled testing approach that spans the full range of possible loading conditions. The result of such an approach is a limit curve, which indicates all combinations of normal and shear stress that the adhesive stress can support, allowing us to understand the full range of possible applications.

B. Alignment

Alignment is an important issue when testing adhesives that rely on van der Waals forces, which require intimate contact with a surface. Gecko-inspired adhesives typically have features on the order of 100 µm or smaller, making alignment to

Tested Material	Directions	Protocol	Examples
Natural Gecko			
	Biaxial	Displacement Control	[27], [32]
	Uniaxial: normal	Displacement Control	[1]
Synthetic Nondirectional			
	Uniaxial: normal	Displacement Control	[7], [33], [34]
	Biaxial: normal & shear	Displacement Control	[35]
Synthetic Directional			
	Uniaxial: normal; full gripper	Displacement Control	[28], [29]
	Biaxial: range of angles; full gripper	Displacement Control	[30]
	Biaxial: normal & shear; full gripper	Displacement Control	[31]
	Biaxial: range of angles	Force Control	[36], [37]
	Biaxial: range of angles	Displacement Control	[38]–[40]
	Uniaxial: shear	Displacement Control	[41]–[45]
	Uniaxial: shear	Force Control	[46]
	Biaxial: normal & shear	Displacement Control	[47]–[51]

TABLE I
COMPARISON OF TESTING METHODS REPORTED IN THE LITERATURE

within a few micrometers important for accurate results. For testing of adhesives, there have been two general approaches used in the literature: using a gently curved test surface, and using a flat surface with an adjustment mechanism.

When using a curved surface, typically a section of a sphere is employed, permitting misalignments of a few degrees without change in overall contact conditions. This setup is used by [34], [39], [44], [49], [50], [53] among others. The insensitivity to alignment simplifies setup and lends itself to an automated battery of tests, but introduces a nonuniform pressure across the adhesive. The nonuniform pressure makes it difficult to extract an "ideal" limit curve, so while data from curved test surfaces is useful for comparative studies, it is less useful for the design and engineering of grippers and other applications that employ adhesives over finite flat areas.

Testing against flat surfaces makes sample alignment more challenging but makes extraction of a limit curve in terms of pressure relatively easy. Previous approaches have included passive compliant approaches [35], [40], [45], [46], and precision rotation stages to perform sample alignment [8], [9], [41], [48], [51], [56]. The resulting limit curve represents an upper bound limit on adhesive performance, and is a starting point for analyzing more complex loading geometries [55], [57].

C. Test Trajectory

For displacement-controlled tests, there are two test paradigms commonly presented in the literature: load-pull and load-drag-pull tests (Fig. 1). While the loading trajectory is relevant for both force and displacement control, published measurements with force controlled loading to date have been primarily manual measurements [17], [37], [55], so although all follow some variation of preload and load application methods, the trajectory is not tightly controlled and is not typically described in terms of the load-pull vs. load-drag-pull nomenclature. Some are more clearly analogous to load-drag-pull trajectories [43], [54], but only measure frictional effects. Force controlled test equipment to date has likewise been uniaxial [46] and does not neatly align with the above dichotomy.

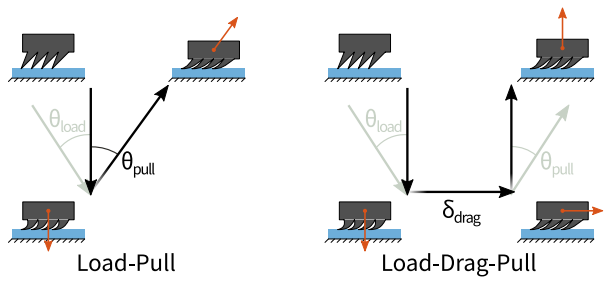

Fig. 1. Illustration of load-pull and load-drag-pull trajectories. Both trajectories load the sample into the test surface along the normal direction (*black arrow*), possibly producing some preload. In the case of the load-pull test, the sample is then pulled away at an angle θ_{pull}, while for the load-drag-pull test the sample is displaced in shear by δ_{drag} before being pulled away in the normal direction. In both tests, the sample may be loaded along an angle θ_{load}, while being pulled away at an angle θ_{pull}, (*gray*). All angles are measured with respect to vertical, clockwise positive.

The load-drag-pull is more common in the adhesion literature [17], [39], and involves bringing the sample into contact along the direction normal to the surface, to a fixed preload depth. This preload depth is either selected in relation to the scale of the wedge features or is selected to correspond to a particular preload pressure. Then, maintaining a constant spacing from the surface, the sample is moved in pure shear to some displacement. The sample is then pulled away from the test surface and the maximum tensile adhesive pressure is recorded.

The load-pull test follows an identical loading trajectory, but then pulls the sample away from the surface at an angle θ_{pull} from vertical without a drag phase.

In general, either of these trajectories may vary both the approach and retraction angles, as in [52], as well as the pulling direction in the contact plane, as in [23], [39].

Both test trajectories can easily be adapted to force controlled testing by applying a pure normal force, then applying a force trajectory—either shear and then normal force, or a combined force directly. In both cases, the relative displacement between the adhesive and the surface is not controlled but allowed to vary; only the resultant force on the adhesive is

controlled. We assume that all forces inside the limit curve are stable, so in the case of force-space testing the results from these two test methods should not be substantially different for quasistatic loading rates.

D. Pull-off Measure

When inspecting a measured force trace, there are multiple methods for determining the failure point. Three that have been used previously are the maximum normal force, maximum force magnitude, and maximum power criteria [56]. We let $\mathbf{f}(t) = \sigma_{\mathrm{s}}(t)\hat{i} + \sigma_{\mathrm{n}}(t)\hat{k}$ be the adhesive stress on the test surface, and let $\mathbf{r}(t)$ be the xz-position of the adhesive with respect to the test stage. The pulloff measures are then given by:

Maximum normal: Failure occurs at $t = \mathrm{argmax}_t\, \sigma_{\mathrm{n}}$.
Maximum magnitude: Failure occurs at $t = \mathrm{argmax}_t \|\mathbf{f}\|$.
Maximum power: Failure occurs at $t = \mathrm{argmax}_t\, \mathbf{f} \cdot \frac{\mathrm{d}\mathbf{r}}{\mathrm{d}t}$.

This last method was shown to provide the best results in displacement controlled load-pull tests [56], as when controlling displacement there may be substantial forces not aligned with the pull-off direction. Ideally, the maximum power method should be used for all displacement controlled testing to account for the fact that the force may be misaligned with the direction of motion. In the particular case of load-drag-pull testing with $\theta_{\mathrm{pull}} = 0$, while the maximum normal force criterion is typically used in the literature, as long as the contact interface does not slip during the drag phase and there is some normal adhesion, we can simplify to $\mathbf{f}(t) \approx C\hat{i} + \sigma_{\mathrm{n}}(t)\hat{k}$ for some constant C. Since the motion during pull $\frac{\mathrm{d}\mathbf{r}}{\mathrm{d}t} = D\hat{k}$, power is maximized when normal stress is maximized, making these methods approximately equivalent. When conducting force controlled testing, the relative motion between the sample and the surface can be hard to know; however, the relative motion is unconstrained, so for quasistatic loading there will be negligible force orthogonal to the direction of applied force. This implies that at the instant of failure, $\mathbf{f}$ is aligned with $\frac{\mathrm{d}\mathbf{r}}{\mathrm{d}t}$, and thus the maximum magnitude method can be used, as it is equivalent to the maximum power method. In the case of uniaxial testing for normal performance, all definitions are equivalent.

III. Test Apparatus Design

Force controlled testing with a flat-on-flat contact is suitable for measuring adhesive performance in a way that corresponds to performance in real-world situations, for example when using an adhesive on flat tiles or film subsrates. However, the predominant approach—namely, testing systems or small samples by manual application of forces—introduces variability in the adhesive loading. Additional factors that make it difficult to generalize the results include the adhesive backing layer stiffness and force alignment with the adhesive area.

To address the limitations of displacement-based testing and manual force-based testing (e.g. load path dependence and sensitivity to loading conditions) we developed a dedicated apparatus for direct force-based testing. By designing this system to be (i) highly stiff in rotational directions but compliant in the translational directions, and (ii) nearly without friction or backlash, the adhesives can be loaded in a highly repeatable manner, producing a force-based adhesive limit surface. This curve can then be adapted to specific applications taking into account the variations in loading conditions present in the application.

A. Architecture

In order to leverage existing displacement controlled testing methods, we choose a series-elastic set of two linear actuators, as illustrated in Fig. 2. The system consists of two linear axes, one to move the test surface in each of the x and z directions with respect to the sample. This is achieved by changing the control positions x_{c} and z_{c}. Once the adhesive is moved into contact with the surface, the output positions x_{o} and z_{o} are nearly constant, to within the characteristic length scale of the adhesive. This results in normal and shear forces applied to the sample through the springs k_{x} and k_{z}.

There are a few critical considerations for such a system. First, as the forces are generated by a series-elastic element, they are not truly constant, but change as the control and output positions change in response to applied forces. The force output resolution is set by the ability to control $x_{\mathrm{c}}, z_{\mathrm{c}}$ and the spring constants k_x, k_z—higher position control resolution and lower spring constants both increase force resolution. The error force is determined by the change in $x_{\mathrm{o}}, z_{\mathrm{o}}$ due to deflection of the adhesive structure; to achieve quasiconstant force, the axis spring constants must be selected low enough for these deflections to result in small forces. Error forces are also created by any friction in the stages, so friction must be minimized. Second, the stage masses m_x and m_y should not be excessive. A mitigating factor is that once the adhesive is in contact, the stages only move by small amounts in the inertial frame. Any rearrangement of the relative configuration of the stages, test surface, and adhesive for fabrication or packaging reasons should preserve this property.

B. Specifications

We designed the apparatus to test patches of adhesive up to 8 mm square with up to 100 kPa pulloff stress in any direction; adhesives with higher limit stresses can be tested using smaller samples. This sample size is selected to be large enough to test adhesive samples with variations over scales much larger than the microscopic feature length. The maximum force is taken to be approximately the maximum force we have tested for PDMS (Sylgard 170, Dow Corning) contact on glass [55], [58]. We assume that the characteristic length scale for motion of the adhesive microstructures is 100 µm, which corresponds to the approximate fibril length used in a variety of adhesives [8], [41], [49]. We further assume that the apparatus only needs to support quasistatic testing, so a moderate system inertia is acceptable. We set a desired maximum error of 1 % of full scale, i.e. 1 kPa. For a sample of the maximum size, the target error corresponds to a force of 64 mN, which sets an upper bound on allowable friction in the axes.

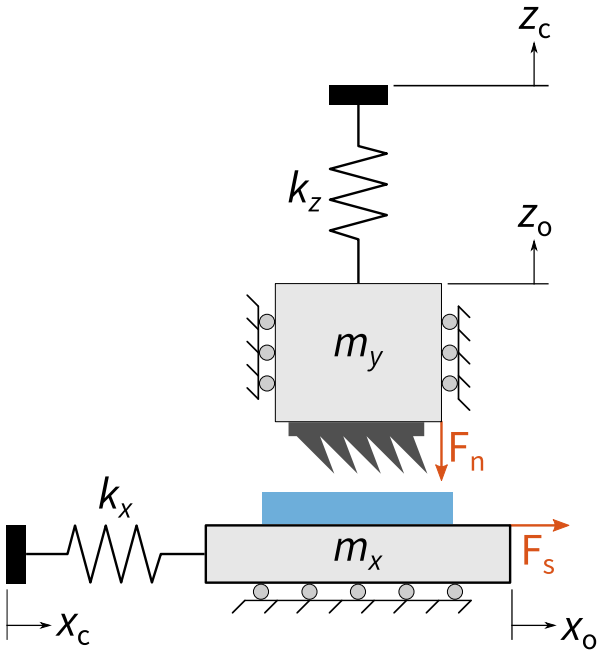

Fig. 2. Schematic of the force-controlled testing system architecture. The adhesive is moved in the x and z directions with respect to the test surface by controlling the stage positions x_c and z_c. Once in contact, the output positions x_o and z_o are nearly constant, to within the characteristic length scale of the adhesive. This results in normal and shear forces applied to the sample through the springs k_x and k_z.

C. Implementation

For minimizing friction and maintaining high off-axis stiffness, we selected linear air bearings to support the stages. As these are non-contact, friction is eliminated entirely, leaving only inertia to affect the motion of the adhesive microstructures. At sufficiently low speeds, this effect is negligible.

The stages were stacked, both supporting the test surface; alignment stages were added to the adhesive, as well as the force sensor. The resulting configuration is shown in Fig. 3. The system is then installed in a CNC machine such that the sample fixture remains fixed in the inertial frame, while the entire crossed-stage assembly is moved into contact with it, reducing required acceleration of the components during a test.

The resulting system meets the performance requirements in the preceding section, and was used to measure limit curve data for a set of representative adhesive materials. See the *supplementary information* for more details on specific component selection, sizing, and characterization of the fabricated apparatus.

IV. Results

We present data measured on flat contacts, as well as on two representative adhesive materials, shown in Fig. 4. For each material, we perform detailed tests in displacement controlled and force controlled modes, using a load-pull trajectory. Force controlled tests are performed with the compliant stage detailed in Section III and Fig. 3, and thus do not globally constrain the relative motion between the sample and the test surface. Displacement controlled tests are performed with the sample held in the same fixture, but tested against a separate, rigid test surface, such that the relative motion in x and z is constrained to that of the motion stage (see Fig. 2 in the *supplementary information*). We also provide comparisons with tests conducted in both modes using load-drag-pull trajectories.

All tests were performed with preload trajectories normal to the surface, with $\theta_{\text{load}} = 0\,^\circ$ as defined according to Fig. 1. See the methods section for details of specific pulloff angles and trajectories used in each test.

We take the z axis to be normal to and away from the adhesive surface, and the x axis in the preferred direction, where applicable. We use the coefficient of adhesion to compare applied preload force required in each test method. For more details on test metrics, see the *supplementary information*.

A. Flat PDMS

As a basic validation that our test methods give reasonable results without the added variable of adhesive geometry effects, we took measurements on a flat sample of silicone (Sylgard 170, Dow Corning) contacting the flat glass test surface (see Fig. 5). All limit surfaces are load-pull trajectories, as a drag-displacement is not expected to affect flat contact measurements but is expected to introduce test artifacts.

As seen in Fig. 5**a**, the shapes of the limit curves are qualitatively similar. However, the preload in DC testing is highly sensitive to preload depth; in this case, 340 kPa at a preload depth of 10 µm, for a factor of adhesion μ' of 0.27. Reducing the preload depth by just 5 µm improves the measured μ' to 0.7, but also changes the limit curve for load states with a shear component. Note also that due to sensitivity of the stiff adhesive material, neither DC test was able to measure points near pure shear.

Force-controlled measurements on the other hand are more uniformly distributed along the limit curve and generally preserve the curve shape as the preload changes. For the FC measures, the measured μ' are 1.4 and 2.5 for the high and low preload cases respectively. In addition, FC testing is able to extend the limit curve to conditions of pure shear.

Figures 5**b** and 5**c** show the measured forces as a function of time for displacement controlled and force controlled tests respectively. The tests were selected to be of comparable measured angle, as defined by the ratio of σ_s to σ_n; in this case, approximately 25 ° to 30 °. The corresponding trajectory angles are 70 ° (b) and 18 ° (c). The offset in measured and trajectory angles for the FC test is as expected due to the initial preload force; for an illustration of these offsets between trajectory and measured angles, refer to Fig. 3 of the *supplementary information*.

Looking at the plots of force as a function of time, we see that the stiffness of the flat PDMS contact causes a slowly varying linear commanded displacement to result in large forces on the sample, with fast, nonlinear loading rates. While less of a problem with microstructured adhesives with lower effective modulus, this phenomenon is still present, and has the potential to introduce rate-dependent effects. Unlike when measuring JKR contacts to develop tribological models—or

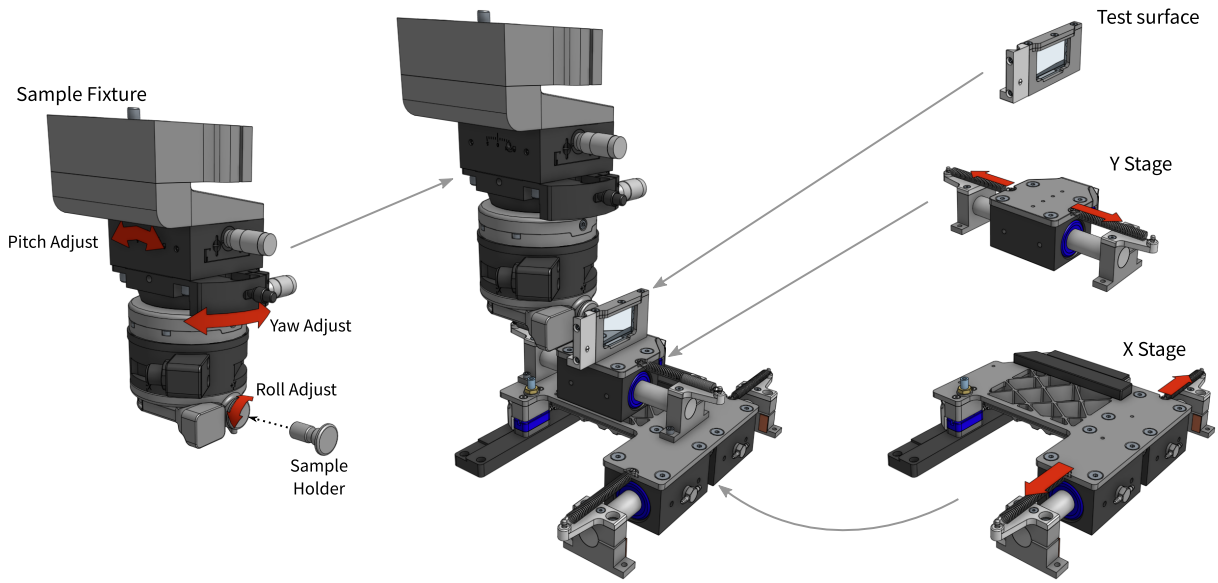

Fig. 3. Illustration of the system. The adhesive sample is affixed to a sample holder and clamped in the sample fixture, which is then clamped to the CNC machine spindle. The sample in-plane rotation (roll) is adjusted by orienting the sample holder prior to clamping it into the fixture. The sample plane is then aligned to the test surface with two fine-adjustment angular stages in the fixture. Motion of the sample fixture brings the sample in contact with the test surface. The test surface is supported by crossed passive elastic stages, allowing motion in the X and Y directions with respect to the machine coordinates. Each stage is supported by air bushings, with an additional planar bearing to fully restrict five degrees of freedom. Air bearing components are in dark blue. Each stage is centered by a pair of springs, visible in the figure under the red arrows indicating stage motion.

even when measuring uniaxial tension on symmetric structured adhesives—the relationship between commanded and effective load rates is determined not only by material properties and contact mechanics, but also by the kinematics of the microstructure deformation. Particularly when measuring adhesives in combined load states, this nonlinearity introduces effects that are difficult to isolate.

In comparison, for FC testing (Fig. 5**c**) the applied forces match the commanded forces on the sample. This better approximates a quasistatic condition, and ensures that while the adhesive structures may be undergoing complex deformations, the applied force does not change in an unpredictable way.

From an applications perspective, the FC data are expected to be more representative, as the majority of reported applications of gecko-inspired adhesive have applied forces. While the DC test parameters can be modified to achieve a limit curve that matches, the natural modifications result in an unrealistic loading process. For instance, the trends in Fig. 5 suggest that increasing the preload in the DC tests or reducing the preload in the FC tests can further align the two data sets. Likewise, increasing the load rate in the DC test would also increase the measured failure points. However, all of these modifications, while aligning the measured outputs, only make the test conditions more mismatched, whether in preload pressure or in loading rate. While this mismatch in test conditions is not necessarily bad in all cases, as we see in the following sections it can become critical depending on the application. Thus, for any testing performed in DC, the results should be carefully validated against the observed behavior in applications.

The model curve presented for comparison is the theoretical limit as predicted by the Eason-Xu-Needleman traction function developed in [58]. In this case, there is a clear discrepancy between the measured data and the adhesive model. The discrepancy when pulling off in the pure normal direction is unlikely to be systematic; plausible values for the material limit of Sylgard 170 with respect to glass vary, and the wedge model for which this traction function was developed is not sensitive to this parameter [58]. The discrepancy in the shear direction is likely to be a systematic issue, reflecting the effects of the finite stiffnesses of the motion stages and test fixture. If we assume that the shear and tensile limits are equal, this implies an approximately 20 % error in the shear measurements. However, the flat-on-flat contact is the worst-case for the test procedure: as a flat sample has maximum stiffness of any adhesive sample, it is therefore the most sensitive to small deflections across the sample. As seen from the displacement controlled data, this sensitivity is enough that even the micron-scale deflections predicted would be enough to substantially change the stress distribution when loaded in shear, thus reducing the total measured force.

As seen in the following sections, when testing fibrillar adhesives the parasitic stage rotations are not an issue and do not reduce the measured adhesive stress. The points on the corresponding limit curves match the results obtained empirically for particular loading directions in applications [22], [55], [57].

B. Microwedge Adhesives

To investigate the effects of test method on the apparent limit surfaces of microstructured gecko-inspired adhesives, we begin by considering the measured performance of wedge-like controllable adhesives developed and used in [8], [22], [55], and shown in Fig. 4**b**. Microwedge adhesives were

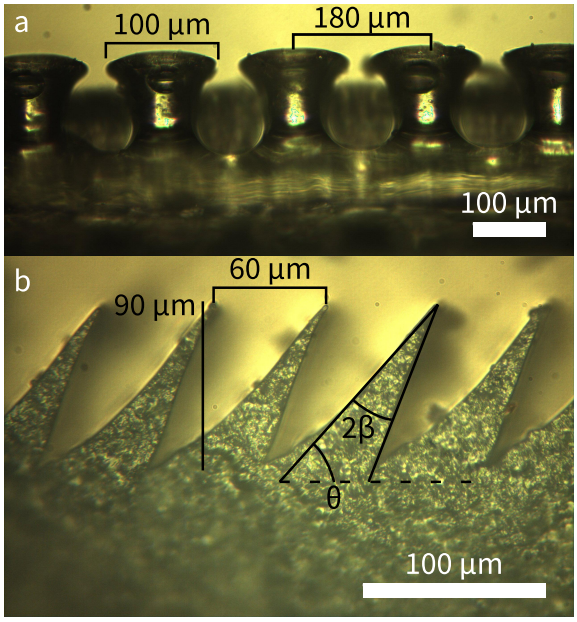

Fig. 4. Microscope images of the representative gecko-inspired adhesives tested. **a:** a commercially-available material (Setex DA 110C, nanoGriptech), which is most similar in geometry to those reported in [7], [49], and of the same class as those reported in [35], [39], [48], [50], having a series of pillars with flat caps on the tips. Caps are 100 µm in diameter and spaced at 180 µm in a hexagonal array. **b:** microindented adhesives first reported in [8], and broadly representative of a growing array of gecko-inspired adhesives designed for anisotropic performance, having asymmetric wedge-like features, shown here in cross section. Wedges are spaced at 60 mm, are 90 µm in height, have half-angle $\beta = 7.5\,^\circ$, and the contacting faces are inclined with respect to the adhesive by $\theta = 52\,^\circ$

manufactured using the micromachining, sculpting and casting procedures detailed in [8], [59]. Flat samples were manufactured by casting a thin film on a polished glass surface. All adhesives were cast with Dow Corning Sylgard 170; this and other polydimethylsiloxane (PDMS) polymers have been used in many gecko-inspired adhesives, particularly directional ones, in part due to their relatively low hysteresis [60], [61]. All data presented in this section were measured on a single sample to eliminate intersample variation and isolate effects due to the testing method. No degradation of the adhesive performance was observed over the course of testing.

Figure 6 shows data measured using a load-pull trajectory; at top using displacement control at several preload displacements; center using force control at several preload pressures; and at bottom a direct comparison of the two test control methods. For the DC tests, the data at 40 µm and 50 µm preload were both taken for the full set of trajectory pulloff angles from 0 ° to 90 °. However, we see that in both cases, the full limit curve cannot be measured; in the case of 40 µm preload depth, we can only reach a measured pulloff angle of 63 °; increasing the preload to 50 µm, we see that this approaches 77 °, still well away from a measurement at 90 °. Further preload to 53 µm is required to measure points at pure shear. This dependence on preload depth is not merely an inconvenience, but rather a fundamental constraint on testing—in order for a displacement controlled test to measure a point near shear, the preload depth necessarily must be at least as far as the wedges deflect under applied shear load. However, for any load trajectory that does not match the natural motion of the wedges, this will introduce a large preload force. For instance, although the measured preload pressure at 40 µm is a reasonable 31 kPa, this increases to 108 kPa at 50 µm, and 154 kPa at 53 µm. This testing protocol results in an apparent μ' of merely 0.12.

By considering the FC data, we see that this apparently low factor of adhesion is an artifact of the test setup. With FC testing, adhesive performance is in fact independent of preload; further, we can measure the adhesive in the low-preload conditions in which it has often been used [22], [57], [62]. When measuring with a nominal preload of 5 kPa, while the measured preload of 6.6 kPa differs slightly due to small calibration offsets of the stage,the resulting μ' is still substantially higher, at 2.5. Not only is the test method more reflective of the application use conditions, but the data are more uniformly distributed along the limit curve, particularly for high-shear loads.

Comparing the two methods (Fig. 6c), we see that the overall shape is comparable. Both tests result in similar pulloff forces at zero shear; however, while testing in displacement control is roughly comparable for moderate shear loads, it diverges at high shear, underestimating the shear limit by approximately 12 %. This is where we should expect the difference to be greatest; the high-shear condition is precisely the point at which the adhesive performance is most dependent on the particular details of the geometric deformation. The *supplementary information* provides a general approach for comparing limit curves with uncertainty in both normal and shear stresses.

The difference in test metrics becomes more pronounced in the reverse direction. Figure 7 shows the full limit curve of pulloff angles from -90 ° to 90 ° of the microwedge adhesive as measured by FC and DC load-pull tests. The displacement control test in this case shows an apparent lack of adhesion in the reverse direction, in this case the result of interactions between the loading trajectory and the adhesive microstructure. Indeed, it shows what looks like the left side of a Coulomb friction cone, like that reported by Autumn *et al.* for gecko adhesion [63] and for an early version of directional polymer stalks [20]. The force-controlled test instead reveals a shear limit that is nearly the same in the reverse direction as in the preferred direction for this adhesive.

For this adhesive, when tested in FC, the wedges are free to flip over and contact on the reverse faces. In this condition, the local contact geometry is nearly identical to that in the preferred direction, and so apart from slightly increased strain energy in the wedges, the adhesion properties are similar. DC testing, as it constrains the motion of the wedges, does not permit this deformation, and so does not measure increased adhesion.

This behavior is borne out in systems-level observations of grasping with microwedge adhesives [23]. While the equal shear stress magnitudes are not expected to generalize to other anisotropic adhesives with different geometries, it serves as a stark illustration of the difference between the two test methods.

Figure 8 shows a comparison of limit curves measured

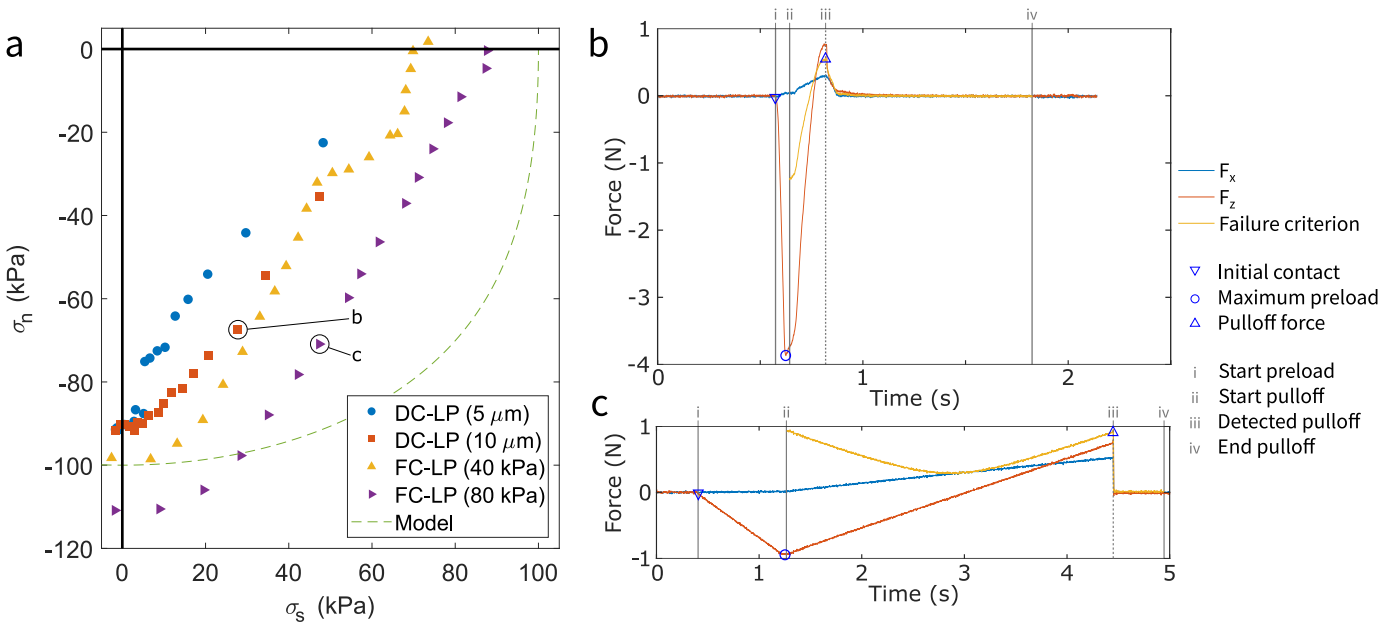

Fig. 5. Comparison of data from force-controlled (FC) and displacement-controlled (DC) load-pull (LP) testing of flat PDMS on glass. **a** shows full limit curves measured with each method; **b** (DC, $\theta_{\text{pull}} = 70\,^\circ$) and **c** (FC, $\theta_{\text{pull}} = 18\,^\circ$) show normal and shear forces versus time for the tests (b) and (c), labeled in **a**. Tests progress from initial contact (i) to maximum compressive preload (ii), through detected pulloff (iii). As seen in **a**, DC data are spaced nonuniformly along each limit curve, while the FC data are more evenly spaced. This is partly due to the fact that in DC, the preload force is necessarily high, and both preload and pulloff forces are rapid and nonlinear. FC tests result in smoother force application, with the load rate easily controlled. DC testing also requires these high preload forces to measure near pure shear; FC tests allow substantially lower preloads that are controlled independently of pulloff angle.

using load-drag-pull trajectories, as is more common in the literature [39]. In this case, while the FC data are reasonably close to the data obtained with an FC load-pull trajectory (Fig. 6), the DC data are markedly higher in the preferred direction than both DC and FC load-pull data. Again, the DC data do not fully support the limit curve, while the FC data do; the difficulty is again in measuring points near shear with the DC test. As was the case for Fig. 6, a very high preload—which would not be used in most applications—was necessary to obtain a curve that extends to the maximum shear case. Additionally, the DC data were measured with a shear drag displacement range of -300 µm to 350 µm, comparable to the maximum required displacement of 350 µm to measure the full limit curve when using a DC load-pull method. That is, even though the drag distance is at least as much as the total motion during the load-pull test, the data are markedly different. This suggests that where shear motion of the adhesive is necessary to activate the adhesive [8], [26], [37], [64] the DC load-drag-pull trajectory may not be a useful test trajectory, even though it is commonly used.

Finally, we compare the effect of trajectory when performing force control testing. Figure 9 shows data plotted for FC tests using both load-pull and load-drag-pull trajectories, conducted with a preload pressure of 10 kPa. Both cases match well, apart from the region near the maximum preferred shear point. This difference may be due to the adhesive itself, as a similar effect has been observed for microwedge adhesives in Fig. 5.13 of [58].

C. *Capped Pillars*

To validate force controlled testing as useful for a broader class of adhesives, we conducted tests on a second commonly used class of gecko-inspired adhesives, those involving the adhesion of pillars to a substrate, possibly with caps on the ends. For ease of procurement and consistency of the adhesive geometry, we used a commercially available gecko adhesive, shown in Fig. 4**a**. These adhesives are most similar in geometry to those reported in [7], [49], and similar to those reported in [35], [39], [48], [50]. Unlike the controllable microwedge adhesives, this class of adhesives provides substantial adhesion at zero friction, as well as typically requiring higher preload forces to fully engage. These properties make this class of adhesives well suited for different tasks than the directional adhesives.

The capped pillar features in the Setex adhesive are arranged in a hexagonal close-packed arrangement. For testing, we define the x axis to be along a row of pillars, making the geometry, and therefore limit curve, symmetric about the z axis.

Figure 10 shows a comparison of limit curves measured using load-pull trajectories in displacement control (*left*), force control (*center*), and a direct comparison (*right*). In each case, several preload values were tested. As expected, these adhesives show a strong dependence on preload in both cases. Visually, the FC limit curves all appear to be smoother, although without a justified basis function this cannot be shown statistically. The comparison plot at right compares the FC data taken at 80 kPa nominal preload to the DC data taken at 20 µm, which results in comparable measured preload stresses of 85 kPa and 95 kPa respectively. Note that the FC load-pull

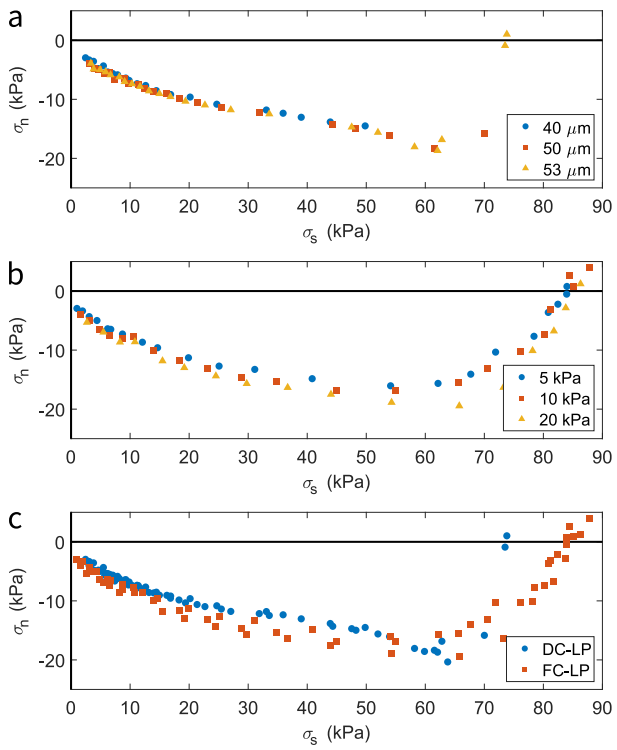

Fig. 6. Comparison of microwedge adhesive limit curves using a load-pull trajectory in both displacement and force control modes with varying preload. $\theta_{\text{load}} = 0\,^\circ$, $\theta_{\text{pull}} \in [0\,^\circ, 5\,^\circ, \ldots, 80\,^\circ, 85\,^\circ, 86\,^\circ, 87\,^\circ, 88\,^\circ, 89\,^\circ]$ **a:** When controlling displacement, although the same range of pulloff angles were used for all preloads, the angle of the measured failure point is coupled to the preload; necessarily, measurements near pure shear have very high preload force. **b:** When controlling forces, varying the preload has no measurable effect on the microwedge limit curve, allowing testing in the low-preload high-shear regime these adhesives are developed for. **c:** Direct comparison of the aggregate limit curves for each control mode; note that displacement controlled data are sparse near shear, as the resultant force is sensitive to small changes in displacement.

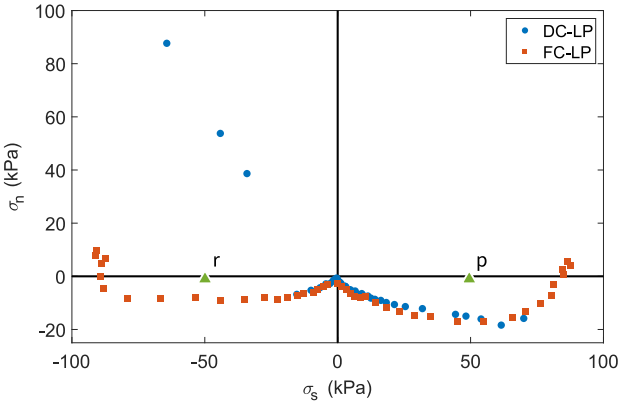

Fig. 7. Comparison of microwedge limit curves using DC load-pull (DC-LP) tests at 50 µm preload, and FC load-pull (FC-LP) tests at 10 kPa preload. While DC testing appears to indicate Coulomb friction behavior in the reverse direction,FC testing indicates that adhesion is present. Points *p* and *r* correspond to the hanging plate demonstration in Fig. 12 in the "preferred" and "reverse" direction, respectively. While both DC and FC testing show that *p* is supported, DC testing would predict that upside-down hanging (*r*) is not.

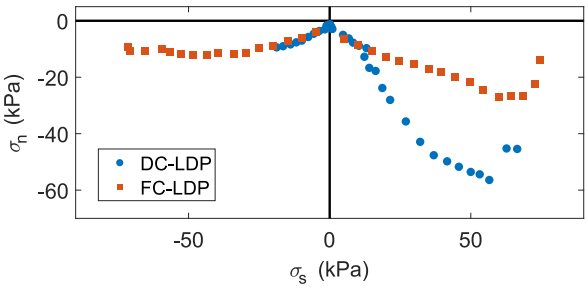

Fig. 8. Comparison of microwedge limit curves using DC load-drag-pull (DC-LDP) tests at 50 µm preload, and FC load-drag-pull (FC-LDP) tests at 10 kPa preload. FC-LDP matches qualitatively the data from FC-LP testing. However, DC-LDP testing yields apparently high normal stresses, which are not observed in practice. Even when the drag distances are significantly longer than the wedge scale, measurements near pure shear are not accessible in either the forward or reverse directions for DC testing.

test measures a limit curve with 100 kPa peak normal, and the DC load-pull test measures a curve with 80 kPa peak normal—not only does the DC test measure a lower reported number, it does so at a higher applied preload force. In this case, the factors of adhesion are 1.18 and 0.84 for the FC and DC tests respectively.

Figure 11 shows a comparison of testing the adhesive sample using both trajectory control methods but in a load-drag-pull test. These tests are performed at the same preloads as in Fig. 10, *right*. Given that a load-drag-pull test with zero shear displacement is equivalent to a load-pull test with zero pulloff angle, we see that the normal stress capability is equal to that measured with the load-pull test. In the case of testing the adhesive using a load-drag-pull trajectory, however, we see that the normal adhesion that was available when pulling towards high shear stress in the load-pull test is not available when performing the drag and pull separately. We hypothesize that this is due to the differing behavior of the mushroom caps under shear loading under compressive vs. tensile loading. Imaging performed on similar geometries in [35] shows that at large shear forces, the ends of the adhesive features detach, and the shear force is supported by the sides of the pillars. In this configuration, the stored elastic energy releases the adhesive from the surface, and as the applied preload is released the adhesive can be removed with little or no measurable adhesion. Similar behavior is also reported in [39] when performing DC load-drag-pull tests on similar adhesives.

V. Correspondence with Applications

Although a broad comparison with applications is beyond the scope of this paper, we present a couple of examples that highlight the differences in predicted behavior from

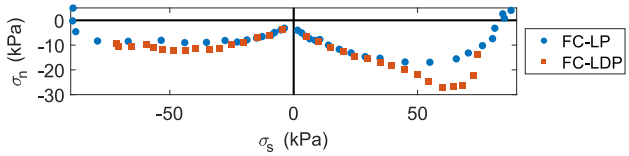

Fig. 9. Comparison of measured microwedge limit curves using FC load-pull (FC-LP) and FC load-drag-pull (FC-LDP) with a 10 kPa preload. Both measured limit curves agree qualitatively, and remaining differences may be explained by path dependence inherent in the adhesive behavior. Either test is likely to give accurate results depending on which is better aligned with the target adhesive conditions.

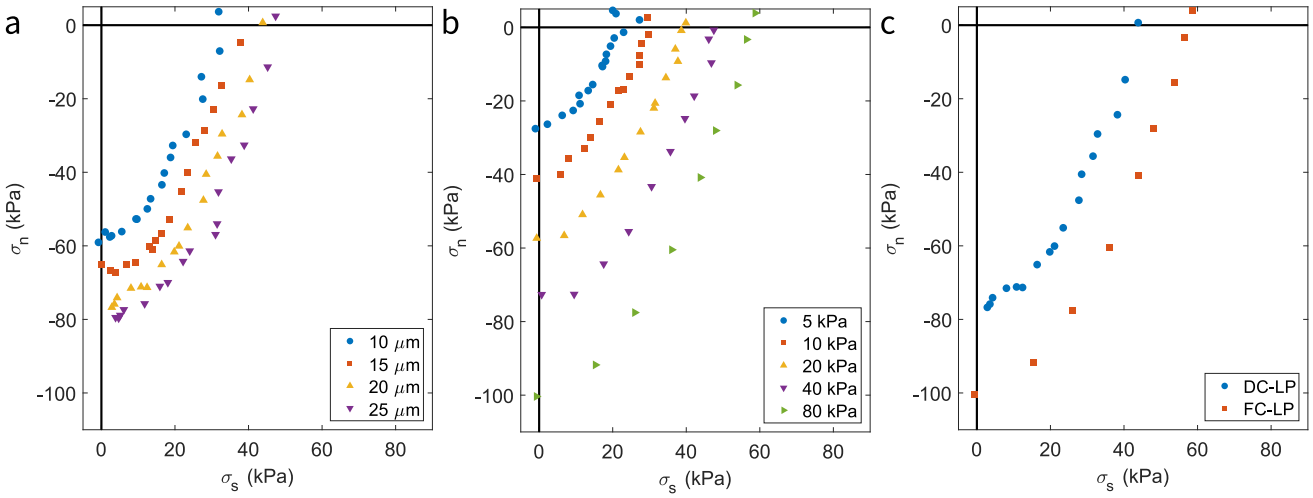

Fig. 10. Comparison of capped pillar adhesive limit curves in both displacement and force control modes with varying preload using load-pull trajectories. **a:** DC testing for capped pillars can measure failure points near pure shear, but the spacing of data along the limit curves is again variable as for the microwedge adhesives. **b:** FC testing, as for microwedge adhesives, results in data that are more evenly spaced, corresponding to the intended test direction. Unlike the microwedge adhesives, these adhesives do inherently have a dependence on preload, which is reflected in the data. **c:** Direct comparison of the aggregate limit curves for each control mode, at equivalent preloads.

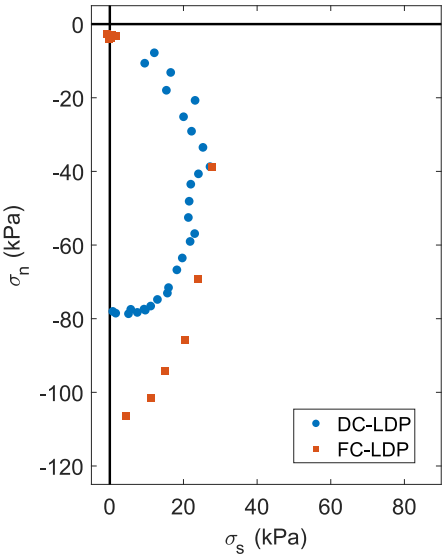

Fig. 11. Comparison of capped pillar limit curves using load-drag-pull trajectories using DC at 25 µm preload and FC at 80 kPa preload. As for load-pull testing, the displacement control mode significantly underestimates the available adhesion. Both testing methods indicate negligible adhesion for effective shear stresses above about 30 kPa; this is a known property of the adhesive structure, where sufficient shear stress while under compression causes the caps to detach from the surface.

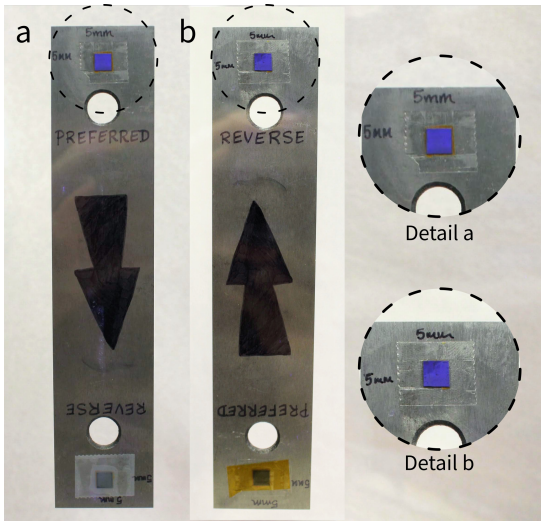

Fig. 12. A steel plate is supported on a vertical glass surface by microwedge adhesives operating in the preferred direction (**a**), and in the reverse direction (**b**). Approximate shear load is 50 kPa, which is near the point of maxium adhesion in both directions. The limit curve measured using displacement control would suggest that adhering in the reverse direction (**b**) is not possible. (Fig. 7).

displacement-controlled and force-controlled testing. The most dramatic differences for directional adhesives are apparent when they are loaded in the reverse or non-preferred direction.

Figure 12 shows a steel plate with a mass of 117 g, and attached adhesive patches of $5\,mm \times 5\,mm$, oriented in the same direction at the top and bottom. The plate was adhered to a vertical glass plate using only the upper adhesive patch, with a piece of smooth tape preventing adhesion from the lower patch. The figure shows the two orientations "right side up," which loads the adhesive in the preferred direction and "upside down," which loads it in the reverse direction. The shear load in either case is about 50 kPa and the normal stress is about -1 kPa . In both cases the glass was edge-lit to produce a frustrated total internal reflection (FTIR) image of the contact area [23], [65]. The plate is supported in both orientations, but the corresponding shear and normal stresses, denoted by labels p and r in Fig. 7, show that only FC testing predicts this result.

For a less carefully aligned example, we created a "backwards" version of the flexible film gripper described in [22]. As seen in Fig. 13, the film gripper is able to lift a football with the adhesives in either the preferred or non-preferred direction, consistent with the FC limit curve in Fig. 7.

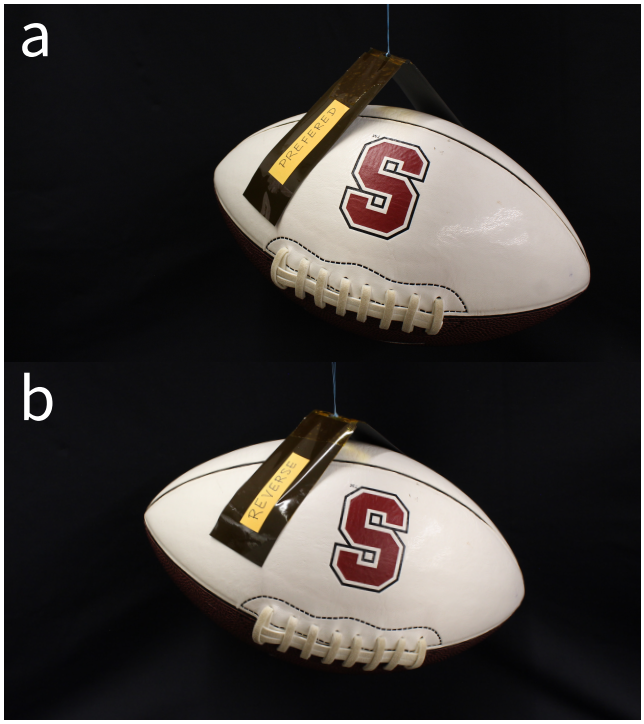

Fig. 13. An American football (392 g) is lifted by a flexible-film gripper with adhesives oriented in the preferred (**a**) and reverse (**b**) directions.

VI. Discussion

A good test method should have two key characteristics. First, it should reflect the conditions that will be experienced by the adhesive in use. Second, it should not introduce bias to the measurement that is a byproduct of the test setup and procedure.

When evaluating the existing adhesive test methods, we see that the first property is rarely the case for the range of testing methods reported in the literature. Apart from exceptional circumstances, applications of gecko-inspired adhesives outside the laboratory do not impose a fixed displacement between the adhesive and the surface. However, the majority of tests reported for gecko adhesives have used displacement controlled tests for measuring the properties of the adhesives. This is not inherently a flaw; while macroscopic objects also typically support applied forces, materials testing conducted in displacement control yields good results. Implicit is the assumption that the measured properties do not depend on the details of the relative motion, but simply the ultimate forces. However, this is not a good assumption when testing gecko-inspired adhesives, which all depend on the specific properties and motion of the microstructure for adhesion.

This mismatch between test and use conditions in adhesive testing introduces additional bias in the form of path dependence. In the case of any of these adhesives, the adhesive structures deform in response to applied loads; if the test method does not permit this deformation, a bias is introduced due to the difference between the commanded and self-deflection paths. In the case of shear adhesives particularly, this couples preload to the ability to measure certain points on the limit curve. Further, as gecko-inspired adhesives are developed with more complex structures to tailor their adhesive properties, even approximations will not be feasible without *a priori* knowledge of the limit curve and the detailed motions of the adhesive structure—not a good prerequisite when testing a novel adhesive. An example of this is the highly anisotropic adhesive presented in [54]; the reverse direction behavior depends not only on the structural motion of the adhesive, but also on nonmonotonic relative displacement between the adhesive and the surface. These discrepancies have not been critical to date because testing has largely been conducted in uniaxial tests, in a specific regime where a displacement controlled approximation is sufficient, or by testing on the actual system directly.

The majority of tests on capped pillar adhesives have been along the z axis; in this case, there is not expected to be a substantial difference between force- and displacement-control testing, as the test trajectory is entirely aligned with the adhesive structure deflection. The time dependence of the force does change, however. For a constant-velocity displacement trajectory, the force will typically change nonlinearly, which may help to explain the difference in normal force measured in Fig. 10.

In the case of previous measurements of shear controlled adhesives, the applications have largely been climbing, perching, or grasping with grippers designed specifically to operate in one shear direction [21], [57], [62], [66]. For these applications, the only critical portions of the limit curve are those where the shear is in the preferred direction. In this quadrant, displacement-controlled tests can provide a good approximation of the adhesive limit curve, as seen in Fig. 6. However, even while the shape of the limit curve is a good match, the preload force imposed by the testing trajectory is coupled to the angle of measurement. While shear adhesives tested to date yield the same performance regardless of preload, this constraint does mean that they cannot be directly tested in the low-preload conditions for which they are most suited.

The other approach in the literature is to test the adhesive limits of an entire system that includes the adhesive, whether mounted on a film, tile, or other carrier. This approach has the benefit of giving results that are directly applicable to the use case but can require the development of test procedures and fixtures that are highly application-specific. Nevertheless, this approach has been used, for example, in [21], [23], [30], [46]. In some cases, testing the full system is necessary to verify performance.

When considering the difference between load-pull and load-drag-pull in FC testing, the answer is again that the test method should be aligned to the expected loading in the application. While load-pull and load-drag-pull tests are easy to implement, the presented test apparatus is capable of following arbitrary loading trajectories.

In summary, FC testing is likely to provide measurements that better match the observed behavior not only for climbing robots but also for new applications including adhesive power transmission with reversing loads [67] and the acquisition of free-floating objects [57], [68]. Applying directional adhesives to industrial grippers [23], [69] requires understanding the preload dependence, as well as adhesion in the non-preferred

direction. Adhesives used in skin-contact [24] will experience complex loading conditions due to the elastic nature of skin. In these applications, the adhesive limit curves captured with the new force-controlled system predict the performance to be obtained in practice, and can help accelerate the transition of gecko-inspired adhesives from laboratory experiments to widespread use.

METHODS

Flat Samples

All flat samples in Section IV-A were tested using a load-pull trajectoryusing $\theta_{\text{load}} = 0\,^\circ$, and $\theta_{\text{pull}} \in [0\,^\circ, 5\,^\circ, \ldots, 80\,^\circ, 85\,^\circ, 86\,^\circ, 87\,^\circ, 88\,^\circ, 89\,^\circ]$. DC tests were performed at preload displacements of 5 µm and 10 µm. FC tests were performed at preload pressures of 40 kPa and 80 kPa.

Microwedge Samples

All microwedge samples in Section IV-B were tested using $\theta_{\text{load}} = 0\,^\circ$.

a) Load-pull Testing: DC tests were conducted using $\theta_{\text{pull}} \in [0\,^\circ, 5\,^\circ, \ldots, 80\,^\circ, 85\,^\circ, 86\,^\circ, 87\,^\circ, 88\,^\circ, 89\,^\circ]$. FC tests were conducted using $\theta_{\text{pull}} \in [0\,^\circ, 5\,^\circ, \ldots, 60\,^\circ, 65\,^\circ, 70\,^\circ, 73\,^\circ, 76\,^\circ, 79\,^\circ, 82\,^\circ, 85\,^\circ, 86\,^\circ, 87\,^\circ, 88\,^\circ, 89\,^\circ]$. In both cases, data points are spaced more closely near shear as the expected adhesive limit curve is more sensitive to pulloff angle in this area. DC tests were performed at preload displacements of 40 µm, 50 µm, and 53 µm. FC tests were performed at preload pressures of 5 kPa, 10 kPa, and 20 kPa.

b) Load-drag-pull Testing: DC tests were conducted using a drag distance $\delta \in$ [-300 µm, -275 µm, ... , -125 µm, -100 µm, -90 µm, ... , 90 µm, 100 µm, 125 µm, ... , 325 µm, 350 µm]. FC tests were conducted using a drag stress $\sigma \in$ [-80 kPa, -75 kPa, ... , 75 kPa, 80 kPa]. DC tests were performed at preload displacement of 50 µm. FC tests were performed at preload pressure of 10 kPa.

Capped Pillar Samples

All capped pillar samples in Section IV-C were tested using $\theta_{\text{load}} = 0\,^\circ$.

c) Load-pull Testing: DC tests were conducted using $\theta_{\text{pull}} \in [0\,^\circ, 5\,^\circ, \ldots, 80\,^\circ, 85\,^\circ]$. FC tests were conducted using $\theta_{\text{pull}} \in [0\,^\circ, 5\,^\circ, \ldots, 80\,^\circ, 85\,^\circ]$. DC tests were performed at preload displacements of 10 µm, 15 µm, 20 µm, and 25 µm. FC tests were performed at preload pressures of 5 kPa, 10 kPa, 20 kPa, 40 kPa, and 80 kPa.

d) Load-drag-pull Testing: DC tests were conducted using a drag distance $\delta \in$ [0 µm, 5 µm, ... , 115 µm, 120 µm]. FC tests were conducted using a drag stress $\sigma \in$ [0 kPa, 5 kPa, ... , 65 kPa, 70 kPa]. DC tests were performed at preload displacement of 25 µm. FC tests were performed at preload pressure of 80 kPa.

Competing Interests

The authors declare no competing interests.

Contributions

S.A.S, M.R.C, and E.W.H. designed research; S.A.S., and E.W.H. performed research; S.A.S. analysed data; S.A.S, A.H.A, M.R.C, and E.W.H. wrote the paper.

Data Accessibility

All data are included in the electronic supplementary material.

Funding

S.A. Suresh was supported in part by a NASA Space Technology Research Fellowship, A. Hajj-Ahmad was supported in part by a NSF Graduate Fellowship. Additional support was provided by the Ford-Stanford Research Alliance and Honda R&D.

REFERENCES

[1] K. Autumn, M. Sitti, Y. A. Liang, A. M. Peattie, W. R. Hansen, S. Sponberg, T. W. Kenny, R. Fearing, J. N. Israelachvili, and R. J. Full, "Evidence for van der Waals adhesion in gecko setae," *Proceedings of the National Academy of Sciences*, vol. 99, no. 19, pp. 12252–12256, 2002.

[2] R. J. Full, K. Autumn, Y. A. Liang, S. T. Hsieh, W. Zesch, W. P. Chan, T. W. Kenny, and R. Fearing, "Adhesive force of a single gecko foot-hair," *Nature*, vol. 405, pp. 681–685, 6 2000.

[3] S. N. Gorb, ed., *Functional surfaces in biology: adhesion related phenomena*, vol. 2. Springer Netherlands, 2009.

[4] S. Gorb, *Attachment Devices of Insect Cuticle*. Dordrecht: Kluwer Academic Publishers, 2001.

[5] S. Gorb, M. Varenberg, A. Peressadko, and J. Tuma, "Biomimetic mushroom-shaped fibrillar adhesive microstructure," *Journal of The Royal Society Interface*, vol. 4, no. 13, pp. 271–275, 2007.

[6] G. Carbone, E. Pierro, and S. N. Gorb, "Origin of the superior adhesive performance of mushroom-shaped microstructured surfaces," *Soft Matter*, vol. 7, pp. 5545–52, 6 2011.

[7] S. Song, D.-M. Drotlef, C. Majidi, and M. Sitti, "Controllable load sharing for soft adhesive interfaces on three-dimensional surfaces," *Proceedings of the National Academy of Sciences*, vol. 114, no. 22, pp. E4344–E4353, 2017.

[8] P. Day, E. V. Eason, N. Esparza, D. Christensen, and M. Cutkosky, "Microwedge Machining for the Manufacture of Directional Dry Adhesives," *J Micro Nano-Manuf*, vol. 1, p. 11001, 3 2013.

[9] A. Parness, D. Soto, N. Esparza, N. Gravish, M. Wilkinson, K. Autumn, and M. Cutkosky, "A microfabricated wedge-shaped adhesive array displaying gecko-like dynamic adhesion, directionality and long lifetime.," *Journal of The Royal Society Interface*, vol. 6, no. 41, pp. 1223–32, 2009.

[10] L. F. Boesel, C. Greiner, E. Arzt, and A. del Campo, "Gecko-Inspired Surfaces: A Path to Strong and Reversible Dry Adhesives," *Advanced Materials*, vol. 22, no. 19, pp. 2125–2137, 2010.

[11] M. Kamperman, E. Kroner, A. del Campo, R. M. McMeeking, and E. Arzt, "Functional adhesive surfaces with "gecko" effect: The concept of contact splitting," *Advanced Engineering Materials*, vol. 12, no. 5, pp. 335–348, 2010.

[12] D. Sameoto and C. Menon, "Recent advances in the fabrication and adhesion testing of biomimetic dry adhesives," *Smart Mater. Struct.*, vol. 19, no. 10, p. 103001, 2010.

[13] M. K. Kwak, C. Pang, H.-E. Jeong, H.-N. Kim, H. Yoon, H.-S. Jung, and K.-Y. Suh, "Towards the next level of bioinspired dry adhesives: new designs and applications," *Advanced Functional Materials*, vol. 21, no. 19, pp. 3606–3616, 2011.

[14] M. Zhou, N. Pesika, H. Zeng, Y. Tian, and J. Israelachvili, "Recent advances in gecko adhesion and friction mechanisms and development of gecko-inspired dry adhesive surfaces," *Friction*, vol. 1, pp. 114–129, 6 2013.

[15] P. M. Favi, S. Yi, S. C. Lenaghan, L. Xia, and M. Zhang, "Inspiration from the natural world: from bio-adhesives to bio-inspired adhesives," *Journal of Adhesion Science and Technology*, vol. 28, no. 3-4, pp. 290–319, 2014.

[16] D. Sameoto, "Manufacturing Approaches and Applications for Bioinspired Dry Adhesives," in *Bio-inspired Structured Adhesives: Biological Prototypes, Fabrication, Tribological Properties, Contact Mechanics, and Novel Concepts* (L. Heepe, L. Xue, and S. N. Gorb, eds.), pp. 221–244, Cham: Springer International Publishing, 2017.

[17] J. Eisenhaure and S. Kim, "A Review of the State of Dry Adhesives: Biomimetic Structures and the Alternative Designs They Inspire," *Micromachines*, vol. 8, no. 4, 2017.

[18] M. P. Murphy and M. Sitti, "Waalbot: An agile small-scale wall-climbing robot utilizing dry elastomer adhesives," *IEEE/ASME transactions on Mechatronics*, vol. 12, no. 3, pp. 330–338, 2007.

[19] M. P. Murphy, C. Kute, Y. Mengüç, and M. Sitti, "Waalbot II: Adhesion recovery and improved performance of a climbing robot using fibrillar adhesives," *The International Journal of Robotics Research*, vol. 30, no. 1, pp. 118–133, 2011.

[20] S. Kim, M. Spenko, S. Trujillo, B. Heyneman, D. Santos, and M. R. Cutkoskly, "Smooth vertical surface climbing with directional adhesion," *IEEE Transactions on Robotics*, vol. 24, pp. 65–74, 2 2008.

[21] E. W. Hawkes, E. V. Eason, D. L. Christensen, and M. R. Cutkosky, "Human climbing with efficiently scaled gecko-inspired dry adhesives," *Journal of The Royal Society Interface*, vol. 12, no. 102, p. 20140675, 2015.

[22] E. W. Hawkes, H. Jiang, D. L. Christensen, A. K. Han, and M. R. Cutkosky, "Grasping Without Squeezing: Design and Modeling of Shear-Activated Grippers," *IEEE Transactions on Robotics*, vol. 34, pp. 303–316, 4 2018.

[23] J. P. Roberge, W. Ruotolo, V. Duchaine, and M. Cutkosky, "Improving Industrial Grippers with Adhesion-Controlled Friction," *IEEE Robotics and Automation Letters*, vol. 3, pp. 1041–1048, 4 2018.

[24] Q. Li, "A practical fabrication method of the gecko-inspired easy-removal skin adhesives," *Biosurface and Biotribology*, vol. 3, no. 2, pp. 66–74, 2017.

[25] J. Davis, ed., *Tensile Testing*. Materials Park, OH: ASM International, 2 ed., 2004.

[26] K. Autumn and J. Puthoff, "Properties, Principles, and Parameters of the Gecko Adhesive System," in *Biological Adhesives* (A. M. Smith, ed.), pp. 245–280, Cham, Switzerland: Springer International Publishing, 2 ed., 2016.

[27] G. C. Hill, D. R. Soto, A. M. Peattie, R. J. Full, and T. Kenny, "Orientation angle and the adhesion of single gecko setae," *Journal of the Royal Society Interface*, vol. 8, no. 60, pp. 926–933, 2011.

[28] E. W. Schaler, D. Ruffatto, P. Glick, V. White, and A. Parness, "An electrostatic gripper for flexible objects," in *IEEE International Conference on Intelligent Robots and Systems*, vol. 2017-Septe, pp. 1172–1179, Institute of Electrical and Electronics Engineers Inc., 12 2017.

[29] M. Dadkhah, Z. Zhao, N. Wettels, and M. Spenko, "A self-aligning gripper using an electrostatic/gecko-like adhesive," in *2016 IEEE/RSJ International Conference on Intelligent Robots and Systems (IROS)*, pp. 1006–1011, 10 2016.

[30] A. Parness, "Testing Gecko-Like Adhesives Aboard the International Space Station," in *AIAA SPACE and Astronautics Forum and Exposition*, Orlando, FL: AIAA, 2017.

[31] M. Modabberifar and M. Spenko, "Development of a gecko-like robotic gripper using Scott–Russell mechanisms," *Robotica*, vol. 38, no. 3, pp. 541–549, 2020.

[32] N. Gravish, M. Wilkinson, and K. Autumn, "Frictional and elastic energy in gecko adhesive detachment," *Journal of The Royal Society Interface*, vol. 5, no. 20, pp. 339–348, 2008.

[33] V. Tinnemann, L. Hernández, S. C. L. Fischer, E. Arzt, R. Bennewitz, and R. Hensel, "In Situ Observation Reveals Local Detachment Mechanisms and Suction Effects in Micropatterned Adhesives," *Advanced Functional Materials*, vol. 29, p. 1807713, 4 2019.

[34] C. Greiner, A. del Campo, and E. Arzt, "Adhesion of Bioinspired Micropatterned Surfaces: Effects of Pillar Radius, Aspect Ratio, and Preload," *Langmuir*, vol. 23, no. 7, pp. 3495–3502, 2007.

[35] B. Murarash and M. Varenberg, "Tribometer for in situ scanning electron microscopy of microstructured contacts," *Tribology Letters*, vol. 41, pp. 319–323, 2 2011.

[36] D. Ruffatto and M. Spenko, "Parameter optimization of directional dry adhesives for robotic climbing and gripping applications," in *2012 IEEE International Conference on Robotics and Automation*, (St. Paul, MN), pp. 1187–1192, IEEE, 2012.

[37] L. Qu, L. Dai, M. Stone, Z. Xia, and Z. L. Wang, "Carbon nanotube arrays with strong shear binding-on and easy normal lifting-off.," *Science (New York, N.Y.)*, vol. 322, no. 5899, pp. 238–242, 2008.

[38] D. Soto, *Force space studies of elastomeric anisotropic fibrillar adhesives*. PhD thesis, Stanford University, 2010.

[39] Y. Wang, S. Lehmann, J. Shao, and D. Sameoto, "Adhesion circle: A new approach to better characterize directional gecko-inspired dry adhesives," *ACS Applied Materials and Interfaces*, vol. 9, pp. 3060–3067, 1 2017.

[40] J.-K. Kim and M. Varenberg, "Biomimetic wall-shaped adhesive microstructure for shear-induced attachment: the effects of pulling angle and preliminary displacement," *Journal of The Royal Society Interface*, vol. 14, no. 137, p. 20170832, 2017.

[41] K. Jin, J. C. Cremaldi, J. S. Erickson, Y. Tian, J. N. Israelachvili, and N. S. Pesika, "Biomimetic bidirectional switchable adhesive inspired by the gecko," *Advanced Functional Materials*, vol. 24, pp. 574–579, 2 2014.

[42] Y. Park, B. Chen, and R. J. Wood, "Design and Fabrication of Soft Artificial Skin Using Embedded Microchannels and Liquid Conductors," *IEEE Sensors Journal*, vol. 12, pp. 2711–2718, 8 2012.

[43] H. T. Tramsen, S. N. Gorb, H. Zhang, P. Manoonpong, Z. Dai, and L. Heepe, "Inversion of friction anisotropy in a bio-inspired asymmetrically structured surface.," *Journal of the Royal Society, Interface*, vol. 15, p. 20170629, 1 2018.

[44] Z. Wang, "Slanted Functional Gradient Micropillars for Optimal Bioinspired Dry Adhesion," *ACS Nano*, vol. 12, pp. 1273–1284, 2 2018.

[45] A. Simaite, B. Temple, M. A. Karimi, V. Alizadehyazdi, and M. Spenko, "Understanding the influence of silicone elastomer properties on wedge-shaped microstructured dry adhesives loaded in shear," *Journal of the Royal Society Interface*, vol. 15, p. 20180551, 9 2018.

[46] D. Ruffatto, A. Parness, and M. Spenko, "Improving controllable adhesion on both rough and smooth surfaces with a hybrid electrostatic/gecko-like adhesive," *JRSI*, vol. 11, 4 2014.

[47] D. Tao, X. Gao, H. Lu, Z. Liu, Y. Li, H. Tong, N. Pesika, Y. Meng, and Y. Tian, "Controllable Anisotropic Dry Adhesion in Vacuum: Gecko Inspired Wedged Surface Fabricated with Ultraprecision Diamond Cutting," *Advanced Functional Materials*, vol. 27, p. 1606576, 6 2017.

[48] Y. Wang, L. X. Tian, H. Hu, H. Tian, Y. Shao, J. Shao, Y. Wang, X. Li, H. Tian, H. Hu, Y. Tian, and Y. Ding, "Rectangle-capped and tilted micropillar array for enhanced anisotropic anti- shearing in biomimetic adhesion," *J. R. Soc. Interface*, vol. 12, no. 106, 2015.

[49] M. P. Murphy, B. Aksak, and M. Sitti, "Gecko-inspired directional and controllable adhesion," *Small*, vol. 5, pp. 170–175, 12 2009.

[50] W. B. Khaled and D. Sameoto, "Anisotropic dry adhesive via cap defects.," *Bioinspiration & biomimetics*, vol. 8, p. 044002, 10 2013.

[51] J. Tamelier, S. Chary, and K. L. Turner, "Vertical anisotropic microfibers for a gecko-inspired adhesive," *Langmuir*, vol. 28, pp. 8746–8752, 6 2012.

[52] J. Tamelier, S. Chary, and K. L. Turner, "Importance of Loading and Unloading Procedures for Gecko-Inspired Controllable Adhesives," *Langmuir*, vol. 29, pp. 10881–10890, 8 2013.

[53] K. Jin, Y. Tian, J. S. Erickson, J. Puthoff, K. Autumn, and N. S. Pesika, "Design and Fabrication of Gecko-Inspired Adhesives," *Langmuir*, vol. 28, pp. 5737–5742, 4 2012.

[54] S. A. Suresh, C. F. Kerst, M. R. Cutkosky, and E. W. Hawkes, "Spatially variant microstructured adhesive with one-way friction," *Journal of The Royal Society Interface*, vol. 16, no. 150, p. 20180705, 2019.

[55] E. W. Hawkes, H. Jiang, and M. R. Cutkosky, "Three-dimensional dynamic surface grasping with dry adhesion," *The International Journal of Robotics Research*, vol. 35, pp. 943–958, 7 2016.

[56] D. O. Santos, *Contact modeling and directional adhesion for climbing robots*. PhD thesis, Stanford University, 2008.

[57] H. Jiang, E. W. Hawkes, C. Fuller, M. A. Estrada, S. A. Suresh, N. Abcouwer, A. K. Han, S. Wang, C. J. Ploch, A. Parness, and M. R. Cutkosky, "A robotic device using gecko-inspired adhesives can grasp and manipulate large objects in microgravity," *Science Robotics*, vol. 2, p. eaan4545, 6 2017.

[58] E. Eason, *Analysis and measurement of stress distributions in gecko toes and synthetic adhesives*. PhD thesis, Stanford University, 2015.

[59] S. Suresh, D. Christensen, E. Hawkes, and M. Cutkosky, "Surface and Shape Deposition Manufacturing for the Fabrication of a Curved Surface Gripper," *Journal of Mechanisms and Robotics*, vol. 7, no. 2, 2015.

[60] S. O'sullivan, R. Nagle, J. McEwen, and V. Casey, "Elastomer rubbers as deflection elements in pressure sensors: investigation of properties using a custom designed programmable elastomer test rig," *Journal of Physics D: Applied Physics*, vol. 36, no. 15, p. 1910, 2003.

[61] J. C. Lötters, W. Olthuis, P. H. Veltink, and P. Bergveld, "The mechanical properties of the rubber elastic polymer polydimethylsiloxane for sensor applications," *Journal of micromechanics and microengineering*, vol. 7, no. 3, p. 145, 1997.

[62] E. W. Hawkes, D. L. Christensen, and M. R. Cutkosky, "Vertical dry adhesive climbing with a 100x bodyweight payload," in *Proceedings* -

IEEE International Conference on Robotics and Automation, pp. 3762–3769, IEEE, 5 2015.

[63] K. Autumn, A. Dittmore, D. Santos, M. Spenko, and M. Cutkosky, "Frictional adhesion: a new angle on gecko attachment," *Journal of Experimental Biology*, vol. 209, no. 18, pp. 3569–3579, 2006.

[64] J. Lee, R. S. Fearing, and K. Komvopoulos, "Directional adhesion of gecko-inspired angled microfiber arrays," *Applied Physics Letters*, vol. 93, p. 191910, 11 2008.

[65] E. V. Eason, E. W. Hawkes, M. Windheim, D. L. Christensen, T. Libby, and M. R. Cutkosky, "Stress distribution and contact area measurements of a gecko toe using a high-resolution tactile sensor," *Bioinspiration & Biomimetics*, vol. 10, p. 16013, 2 2015.

[66] A. Parness, N. Abcouwer, C. Fuller, N. Wiltsie, J. Nash, and B. Kennedy, "LEMUR 3: A limbed climbing robot for extreme terrain mobility in space," in *2017 IEEE International Conference on Robotics and Automation (ICRA)*, pp. 5467–5473, 5 2017.

[67] N. D. Naclerio, C. F. Kerst, D. A. Haggerty, S. A. Suresh, S. Singh, K. Ogawa, S. Miyazaki, M. R. Cutkosky, and E. W. Hawkes, "Low-Cost, Continuously Variable, Strain Wave Transmission Using Gecko-Inspired Adhesives," *IEEE Robotics and Automation Letters*, vol. 4, pp. 894–901, 4 2019.

[68] M. A. Estrada, B. Hockman, A. Bylard, E. W. Hawkes, M. R. Cutkosky, and M. Pavone, "Free-flyer acquisition of spinning objects with gecko-inspired adhesives," in *Proceedings - IEEE International Conference on Robotics and Automation*, vol. 2016-June, pp. 4907–4913, Institute of Electrical and Electronics Engineers Inc., 6 2016.

[69] M. Guo, D. V. Gealy, J. Liang, J. Mahler, A. Goncalves, S. McKinley, J. A. Ojea, and K. Goldberg, "Design of parallel-jaw gripper tip surfaces for robust grasping," in *Proceedings - IEEE International Conference on Robotics and Automation*, pp. 2831–2838, Institute of Electrical and Electronics Engineers Inc., 7 2017.